HIGH PRESSURE RF CAVITY TEST AT FERMILAB*

B. Freemire†, P.M. Hanlet, D.M. Kaplan, Y. Torun, IIT, Chicago, IL 60616, USA
M.R. Jana, A. Moretti, M. Popovic, A.V. Tollestrup, K. Yonehara, FNAL, Batavia, IL 60510, USA
G. Flanagan, R.P. Johnson, M. Notani, Muons, Inc., Batavia, IL 60510, USA

Abstract

Operating a high gradient radio frequency cavity embedded in a strong magnetic field is an essential requirement for muon beam cooling. However, a magnetic field influences the maximum RF gradient due to focusing of dark current in the RF cavity. This problem is suppressed by filling the RF cavity with dense hydrogen gas. As the next step, we plan to explore the beam loading effect in the high pressure cavity by using a 400 MeV kinetic energy proton beam in the MuCool Test Area at Fermilab. We discuss the experimental setup and instrumentation.

INTRODUCTION

The concept of using muons in colliders or neutrino factories has been around for many years [1, 2]. Ionization cooling allows rapid emittance reduction, with energy restored through radio frequency (RF) cavities. The problem with this scheme is that high gradient RF cavities must be placed in strong magnetic fields (on the order of a few Tesla) [3, 4]. These magnetic fields can focus field emission electrons onto the wall of the cavity, greatly reducing the maximum stable RF gradient [5]. A number of ideas have been proposed to fix this problem, and the MuCool Test Area (MTA) was created partially as an R&D facility for this purpose.

It has been demonstrated that filling an 805 MHz RF cavity with a high pressure gas suppresses breakdown [6]. Tests carried out with a hydrogen gas filled cavity show stable operating gradients on the order of 65 MV/m. Electrodes made of copper, molybdenum, and beryllium were tested without an external magnetic field, and an external field of 3 T was applied with the molybdenum electrodes. Fig. 1 shows the results obtained in these tests. The cavity reached a higher gradient with Molybdenum electrodes. Note there was virtually no difference in maximum gradient attained using the molybdenum electrodes in a 3 T field.

Tests have been performed using different gas species as well. Fig. 2 shows the data taken using a copper electrode with nitrogen, hydrogen, hydrogen with a SF_6 dopant. As can been seen in both Fig. 1 and Fig. 2, there is a region at lower pressures in which the gradient depends linearly on pressure, and a region at higher pressures in which the gradient plateaus and no longer depends on pressure. These are called the Paschen region and metallic region, respectively [7].

A high pressure RF (HPRF) cavity has never been operated with beam before. The effect of beam loading must be investigated. It is thought that ionization electrons will recombine with hydrogen before they can form a dense plasma and degrade the cavity Q. If this is not the case, a dopant electronegative gas will be tested. Nitrogen is a candidate, as it forms ammonia (NH_3) with hydrogen when dissociated. Sulfur hexafluoride (SF_6) is another candidate.

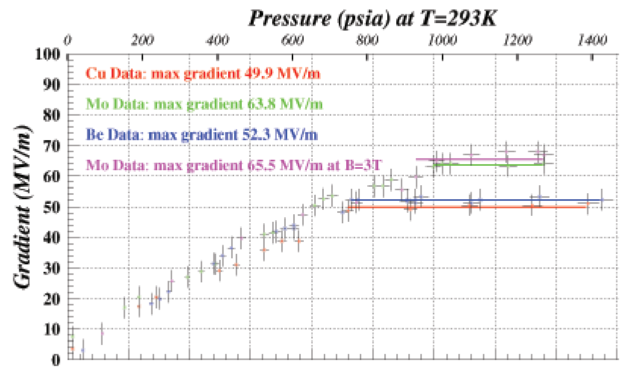

Figure 1: Breakdown gradient with different electrode materials without beam. Copper electrode data is in red, beryllium in blue, molybdenum in green, and molybdenum in a 3 T external magnetic field is in pink [6].

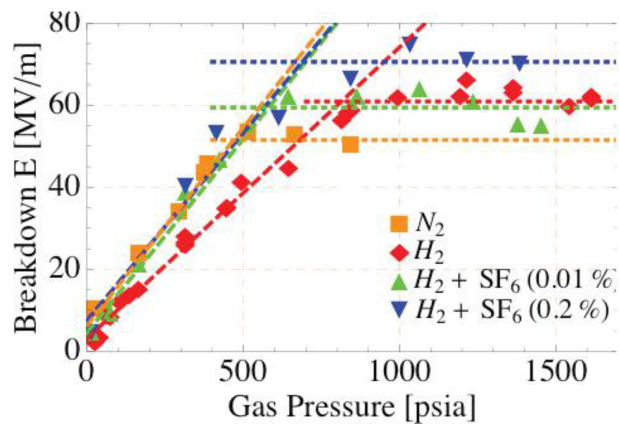

Figure 2: Breakdown gradient for different gas species without beam. Nitrogen is orange, hydrogen blue, hydrogen + SF_6(0.01%) green, and hydrogen + SF_6(0.2%) is blue [8].

MTA EXPERIMENTAL HALL

The MTA experimental hall has been built to accommodate various test programs: RF power is provided at 201 and 805 MHz, high pressure gases including hydrogen up to 1600 psi are available, a 5 T solenoid magnet provides a strong magnetic field, and a proton beamline has been commissioned. Safety issues with regard to the use of pres-

* Work supported in part by grants from the National Science Foundation and the US Department of Energy.
† freeben@iit.edu

surized hydrogen have been addressed, and there is a 15 ft radius around the cavities in which no electrical equipment may be placed.

Beamline

The MTA utilizes the 400 MeV kinetic energy proton beam provided by the Fermilab linac. The allotted 60 pulses per hour deliver 10^{12} to 10^{13} protons per pulse. The final beam intensity is tuned by a collimator placed just upstream of the cavity. The layout of the experimental hall is shown in Fig. 3.

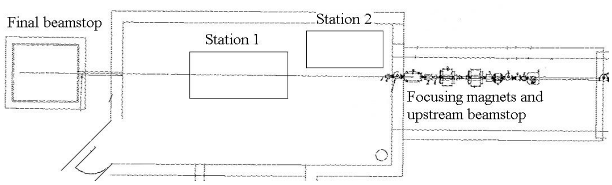

Figure 3: MTA Experimental Hall. RF Station 1 is located inside the solenoid magnet. RF Station 2 is located on a stand upstream and outside of the magnet.

Experimental Apparatus

There are two stations that support RF cavity operation. Station 1 is located in a 5 T, 1.088 m long, 44 cm bore diameter solenoid magnet. The solenoid is on the beamline axis and an extension beampipe ends 1 m from its face. Station 2 is located upstream of the magnet and off the beamline axis. An RF switch has been installed to supply 805 MHz to either station. In order to test the cavity with beam or external magnetic field, the cavity must be located in RF Station 1. RF Station 2 is used for conditioning the cavity and calibrating instrumentation.

The side view schematic for Station 1 operation can be seen in Fig. 4. The beampipe extension is on the left, with a CCD camera (PL-B955U camera) and a Chromox luminescent screen for beam tuning. The two piece stainless steel collimator provides the final beam intensity control, with full or 10% intensity. Two toroids, one before the collimator and one between the collimator and cavity, are used to measure the number of particles incident on the cavity. RF power is fed to the cavity via a waveguide on the downstream side. A beam counter telescope triggers on elastically scattered protons (~360 MeV KE) from the vacuum window at the end of the beampipe. Additionally there are 10 scintillation counters placed in the vacinity of the cavity.

SIGNALS AND INSTRUMENTATION

Each station in the hall is equipped with cabling for electrical and magnetic pickup, forward and reflected power, and optical signals. The cables consist of $\frac{1}{2}$ inch and $\frac{1}{4}$ inch heliax and green RG58. Table 1 shows the type and number of signals provided by each station.

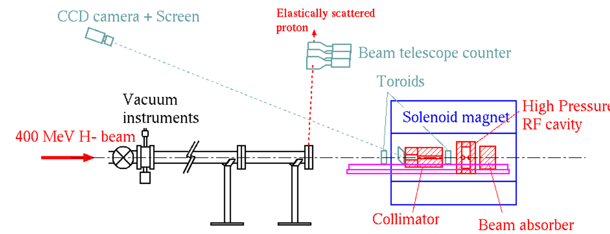

Figure 4: Side view of Station 1 setup. The proton beam comes from the left and passes through the collimator, cavity and beam absorber placed inside the solenoid magnet.

Table 1: Signals per Station

Station	Cable Type	Number of Cables
1	E/M Pickup	2
	For/Ref Power	2
	Optical	3
2	E/M Pickup	2
	For/Ref Power	2
	Optical	6
1 or 2	Spare	9

Calibration

As determining when breakdown occurs during the RF cycle is very important, picosecond timing resolution is necessary. A preliminary timing calibration has been done excluding the cavity, and a more detailed calibration will take place involving the cavity. A laser (PiLas PIL063 laser head and EIG 1000D controller) was used to send light to a Hamamatsu H5783 PMT as a trigger. A signal was also sent through the other instrumentation cables and a Horiba MicroHR Motorized Spectrometer (with a Hamamatsu H5783-20 PMT). The relative delays were measured. Fig. 5 shows the setup and Fig. 6 shows a typical signal delay screenshot. Table 2 lists these cable delays.

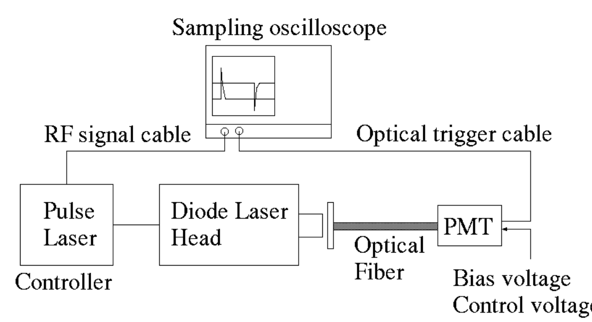

Figure 5: Timing calibration setup. A picosecond laser sends a signal directly to the oscilloscope and through the cables to the scope.

Two ferrite core toroids will be placed on the upstream face of the collimator and between the collimator and cavity. An output signal calibration has been done using a handmade current pulse generator that is based on a fast switching transistor (2N2369A). The current was

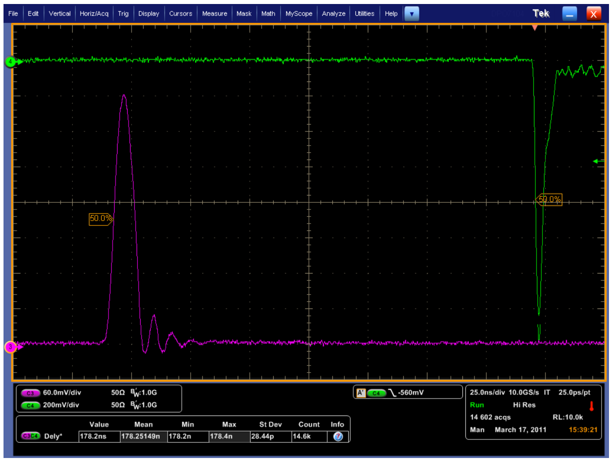

Figure 6: Timing calibration screenshot. The optical signal is in green, and the electrical pickup from Station 1 is in magenta.

Table 2: Cable Delays Relative to PMT Trigger

Station	Cable	Delay
1	1	152.7 +/− 0.3 ns
	2	158.7 +/− 0.2 ns
	3	150.9 +/− 0.2 ns
	4	151.4 +/− 0.4 ns
2	1	182.1 +/− 0.4 ns
	2	182.3 +/− 0.2 ns
	3	181.1 +/− 0.2 ns
	4	181.1 +/− 0.3 ns
Spectrometer		6.9 +/− 0.2 ns

sent through the toroids and the output signal was measured on an oscilloscope. Fig. 7 shows the calibration, 21.26 mV/mA was measured.

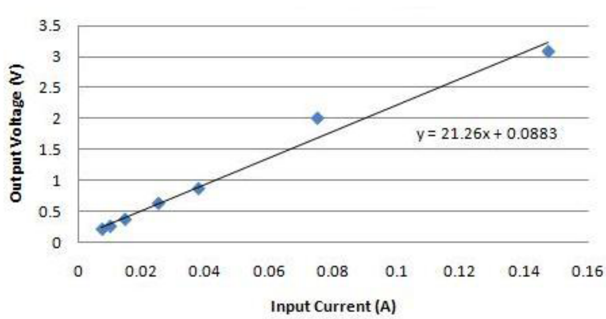

Figure 7: Toroid output voltage versus input current.

DATA ACQUISITION

The data acquisition system consists of two PCs that control the power supplied to the RF cavity and record the various signals. One PC runs a CAMAC and NIM based system. It reads the electrical and magnetic pickup signals, produces an RF envelope and uses the counters to create a trigger. The other PC runs a LabVIEW based system. During conditioning the RF power level is increased every so often until a spark occurs, at which point it decreased and begins to increment again. It uses an external trigger to record resonant frequency, RF envelope, and oscilloscope traces after a specified number of RF cycles. The fast signals (e.g. RF pickups and optical) are fed directly into the oscilloscopes. The slow signals (e.g. RF envelope) are fed into the PCs, which record waveforms from the scopes when a breakdown occurs.

OUTLOOK

Data will soon be taken using the HPRF cavity with and without an external magnetic field, and with and without beam. The results should indicate whether high pressure gases allow RF cavities to be operated in strong magnetic fields with beam.

REFERENCES

[1] D. Neuffer, “Principles and Applications of Muon Cooling,” Part. Accel. 14 (1983) 75, http://lss.fnal.gov/archive/test-fn/0000/fermilab-fn-0378.shtml.

[2] S. Geer, “Neutrino Beams From Muon Storage Rings: Characteristics and Physics Potential,” Phys. Rev. D57 (1998) 6989, http://prd.aps.org/abstract/PRD/v57/i11/p6989_1.

[3] J. Gallardo et al., “$\mu^+\mu^-$ Collider: A Feasibility Study,” DPF/DPB Summer Study on New Directions for High Energy Physics, Snow-mass, Colorado, 25 Jun - 12 Jul 1996, BNL-52503, Fermilab-Conf-96-092, LBNL-38946, http://www.cap.bnl.gov/mumu/pubs/snowmass96.html.

[4] S. Geer, “Muon Colliders and Neutrino Factories,” Ann. Rev. Nucl. Part. Sci. 59 (2009) 347, http://dx.doi.org/10.1146/annurev.nucl.010909.083736.

[5] J. Norem, V. Wu, A. Moretti, M. Popovic, Z. Qian, L. Ducas, Y. Torun and N. Solomey, “Dark Current, Breakdown, and Magnetic Field Effects in a Multicell, 805 MHz Cavity,” Phys. Rev. ST Accel. Beams 6 (2003) 072001, http://prst-ab.aps.org/abstract/PRSTAB/v6/i7/e072001.

[6] P. Hanlet et al, “High Pressure RF Cavities in Magnetic Fields,” EPAC’06, Edinburgh, June 2006, TUPCH147, p. 1364, http://jacow.org/e06/PAPERS/TUPCH147.PDF.

[7] M. BastaniNejad et al, “RF Breakdown of Metallic Surfaces in Hydrogen,” PAC’09, Vancouver, BC, Canada, May 2009, WE5PFP008, p. 2000, http://jacow.org/PAC2009/papers/we5pfp008.pdf.

[8] K. Yonehara et al, “Doped H_2-Filled RF Cavities for Muon Beam Cooling,” PAC’09, Vancouver, BC, Canada, May 2009, TU5PFP020, p. 855, http://jacow.org/PAC2009/papers/tu5pfp020.pdf.

[9] M. R. Jana, “Refurbished Pill Box Data,” MAP Winter Meeting, Jefferson Lab, March 2011, http://conferences.jlab.org/muon2011/index.html.